Neuron
Article

Identification of a Brainstem Circuit Regulating Visual Cortical State in Parallel with Locomotion

A. Moses Lee,[1,2,7] Jennifer L. Hoy,[1] Antonello Bonci,[3,4] Linda Wilbrecht,[5,6] Michael P. Stryker,[7] and Cristopher M. Niell[1,7,*]
[1]Institute of Neuroscience and Department of Biology, University of Oregon, Eugene, OR 97403, USA
[2]Medical Scientist Training Program, Neuroscience Graduate Program, University of California, San Francisco, CA 94158, USA
[3]Intramural Program, National Institute of Drug Abuse, Baltimore, MD 21224, USA
[4]Solomon H. Snyder Department of Neuroscience, Johns Hopkins School of Medicine, Baltimore, MD 21287, USA
[5]Department of Psychology and Helen Wills Neuroscience Institute, University of California, Berkeley, Berkeley, CA 94720, USA
[6]Ernest Gallo Clinic and Research Center, Emeryville, CA 94608, USA
[7]Center for Integrative Neuroscience, Department of Physiology, University of California, San Francisco, San Francisco, CA 94158, USA
*Correspondence: cniell@uoregon.edu
http://dx.doi.org/10.1016/j.neuron.2014.06.031

SUMMARY

Sensory processing is dependent upon behavioral state. In mice, locomotion is accompanied by changes in cortical state and enhanced visual responses. Although recent studies have begun to elucidate intrinsic cortical mechanisms underlying this effect, the neural circuits that initially couple locomotion to cortical processing are unknown. The mesencephalic locomotor region (MLR) has been shown to be capable of initiating running and is associated with the ascending reticular activating system. Here, we find that optogenetic stimulation of the MLR in awake, head-fixed mice can induce both locomotion and increases in the gain of cortical responses. MLR stimulation below the threshold for overt movement similarly changed cortical processing, revealing that MLR's effects on cortex are dissociable from locomotion. Likewise, stimulation of MLR projections to the basal forebrain also enhanced cortical responses, suggesting a pathway linking the MLR to cortex. These studies demonstrate that the MLR regulates cortical state in parallel with locomotion.

INTRODUCTION

Cortical processing is subject to modulation by behavioral state. For example, sensory responses are heavily attenuated during sleep and are often enhanced during states of alertness and attention. In mice, it has been shown that visual responses in the primary visual cortex (V1) dramatically increase while animals are running as opposed to when they are standing quietly alert (Andermann et al., 2011; Ayaz et al., 2013; Keller et al., 2012; Niell and Stryker, 2010). This enhancement of visually evoked responses is accompanied by a shift in the local field potential (LFP) from low frequencies to gamma oscillations (Niell and Stryker, 2010). Recent studies have begun to elucidate the local synaptic mechanisms and effects of neuromodulators that may mediate this effect in cortex (Bennett et al., 2013; Fu et al., 2014; Pinto et al., 2013; Polack et al., 2013). However, the neural circuits that initiate these changes and couple them with locomotor state remain unknown.

In many species, locomotion is mediated by the mesencephalic locomotor region (MLR), defined as the midbrain region in which electrical stimulation is sufficient to induce locomotion at short latencies (Grillner, 2003; Shik et al., 1966). Anatomically, this region loosely coincides with the pedunculopontine tegmental nucleus (PPN) and the cuneiform nucleus in mammals (Mori et al., 1978; Shik et al., 1966). Previous studies in decerebrate preparations have suggested that the MLR is able to regulate gait through descending projections, which can recruit the spinal cord central pattern generators via reticulospinal neurons to initiate locomotion (Grillner et al., 2008; Mori et al., 1978; Shik et al., 1966).

The region around the MLR has also been described as part of the "ascending reticular activating system." Electrical stimulation of this region can induce physiological correlates of alertness, such as desynchronization of low-frequency oscillations (<10 Hz) of the electroencephalogram (Moruzzi and Magoun, 1949), while lesions of this area can elicit a comatose state, abolishing arousal responses to typically salient sensory stimuli (French et al., 1952; Lindsley et al., 1950). Anatomical and functional studies have demonstrated that in addition to its descending projections to motor pathways, the MLR also sends ascending projections to the thalamus and basal forebrain (Nauta and Kuypers, 1958). In turn, activation of the basal forebrain is both necessary and sufficient to induce changes in cortical state and enhancements in sensory responses that are dependent in part on cholinergic neuromodulation (Buzsaki et al., 1988; Goard and Dan, 2009; Hasselmo and Giocomo, 2006; Rodriguez et al., 2004; Sato et al., 1987). Indeed, in a recent study, Pinto et al. (2013) demonstrated that activating cholinergic projections from the basal forebrain into primary visual cortex can recapitulate some of the cortical effects of locomotion.

Clinically, the PPN, an anatomical nucleus within the MLR, is a site for experimental deep brain stimulation (DBS) in patients with Parkinson's disease and other disorders associated with postural and gait dysfunction (Hamani et al., 2011; Stefani et al., 2007). One of the side effects often reported in patients receiving low-frequency DBS in the PPN is the subjective feeling

of "alertness." Thus, numerous lines of scientific and clinical evidence point to the importance of the MLR in regulating behavioral state across species as well as in initiating movements.

Based upon these functional and anatomical considerations, we hypothesized that ascending projections from the MLR to the basal forebrain may mediate changes in cortical processing, while the descending projections initiate locomotion. In this way, the same anatomical region that regulates motor behaviors could also provide a type of efference copy to regulate cortical state. This would be analogous to the coupling of eye movements and spatial attention in primates, where studies have demonstrated that microstimulation in areas involved in orienting motor responses such as the superior colliculus (Cavanaugh and Wurtz, 2004; Müller et al., 2005), frontal eye fields (Armstrong et al., 2006; Moore and Armstrong, 2003; Moore and Fallah, 2001), and lateral intraparietal cortex (Cutrell and Marrocco, 2002) can enhance cortical responses in a manner similar to spatial attention (Bisley, 2011), thereby coupling motor output to attentional shifts in cortical sensory processing. While saccadic eye movements can be initiated by sufficiently high intensities of stimulation in each of these brain regions, changes in cortical response similar to those produced by focal attention can be elicited by subthreshold levels of microstimulation in which no overt movements are made (Armstrong et al., 2006; Moore and Armstrong, 2003; Moore and Fallah, 2001; Müller et al., 2005). This critical choice to use stimulation parameters that were below the threshold for overt saccadic eye movements allowed the experimenters to dissociate changes in visual responses with stimulation from those resulting from eye movements.

We therefore chose to use a similar subthreshold stimulation procedure to study the coupling between motor output and visual processing in the mouse. We found that subthreshold optogenetic stimulation of the MLR was sufficient to increase the gain of visual responses and enhance gamma oscillations similar to those normally associated with locomotion even in the absence of overt movement. Furthermore, stimulation of axon terminals projecting from the MLR to basal forebrain also reproduced this effect, which, combined with recent findings (Pinto et al., 2013; Fu et al., 2014), provides a potential pathway linking activation of the MLR with cortical changes.

RESULTS

Functional Identification of the Mesencephalic Locomotor Region in Mice

The MLR is defined physiologically as the midbrain region where stimulation can reliably induce locomotion at short latencies (Grillner, 2003; Shik et al., 1966). In order to manipulate activity in this region, we targeted bilateral injections of adeno-associated virus (AAV) expressing channelrhodopsin-2 (ChR2) fused to yellow fluorescent protein (eYFP) under the CamK2α promoter into the MLR. After injection, 1 month was allowed to pass to permit expression of ChR2-eYFP prior to additional experiments.

Neurons expressing ChR2-eYFP were visible in the MLR by histology (Figures 1B and 1C). To verify that infected neurons could be optogenetically driven, we performed extracellular silicon multielectrode recordings in the infected region using a previously described apparatus in which a mouse is free to stand, walk, or run on a spherical treadmill while its head is fixed (Dombeck et al., 2007; Harvey et al., 2009; Niell and Stryker, 2010). A fiber optic was placed above the recording site, and 10 ms pulses of blue light were delivered through the fiber. Reliable, short-latency single-unit responses could be elicited within 10 ms to individual light pulses, indicating that we could drive neuronal activity within the area (Figure 1D), although neurons varied in the reliability with which light-evoked responses were elicited. The spike shapes of optically evoked neural responses appeared similar to naturally occurring spikes, suggesting that ChR2 stimulation was not distorting action potentials. While it was clear that light drove the firing of neurons within the infected site, this firing is most likely a mixture of both directly activated ChR2-expressing neurons and synaptically activated downstream partners in the region.

The animal's locomotor behavior was also assessed following optical stimulation. Locomotor speed was registered by optical sensors that measured the rotation of the ball (Dombeck et al., 2007; Niell and Stryker, 2010). Optogenetic stimulation elicited robust locomotion at short latencies from the onset of stimulation, confirming that we were activating neurons within the MLR (Figure 1E; Movie S1).

When we adjusted the intensity of laser stimulation to a point where stimulation at 20 Hz was just sufficient to elicit locomotion reliably, stimulation at 10 Hz usually did not induce overt movement (Figure 1E). This graded locomotor response required a range of peak laser powers across experiments, spanning 0.6 to 5 mW (note that for a 10% duty cycle, the average power delivered to the MLR is 10-fold lower). When locomotion was present during such trains of optogenetic stimulation at 10 Hz, it was highly variable and generally not time locked to the onset of stimulation trains, making it possible to identify epochs with and without optogenetic stimulation when locomotion was either present or absent.

Both the area of infection and placement of the optical fiber determine the area activated by optogenetic stimulation. Post hoc histology was performed to assess the position of the fiber and the presence of viral infection (Figure S1A available online) from experiments where optical stimulation successfully elicited robust locomotion, the signature of activating the MLR. Optical fiber placements were consistently identified within the vicinity of the cuneiform nucleus and PPN, which have classically been associated with anatomical location of the MLR. Infection was also present in neighboring areas associated with auditory processing such as the inferior colliculus, microcellular tegmental nucleus, or inferior nucleus of the lateral lemniscus, but these were distant from the fiber tip. Given the light power used during the experiment and the location of the fiber placements, the behavioral effects elicited by optical stimulation are probably attributable to driving neurons within the PPN, which is a known component of the MLR (Gradinaru et al., 2009).

Because the MLR contains a diverse population of projection neurons, further attempts were made to characterize the population of neurons infected by the virus. When the CamK2α-ChR2-YFP virus was injected into a cross between a VGlut2-cre and tdTomato reporter mouse, virally infected neurons colocalized with tdTomato fluorescence (Figure S1B; 28/32 neurons

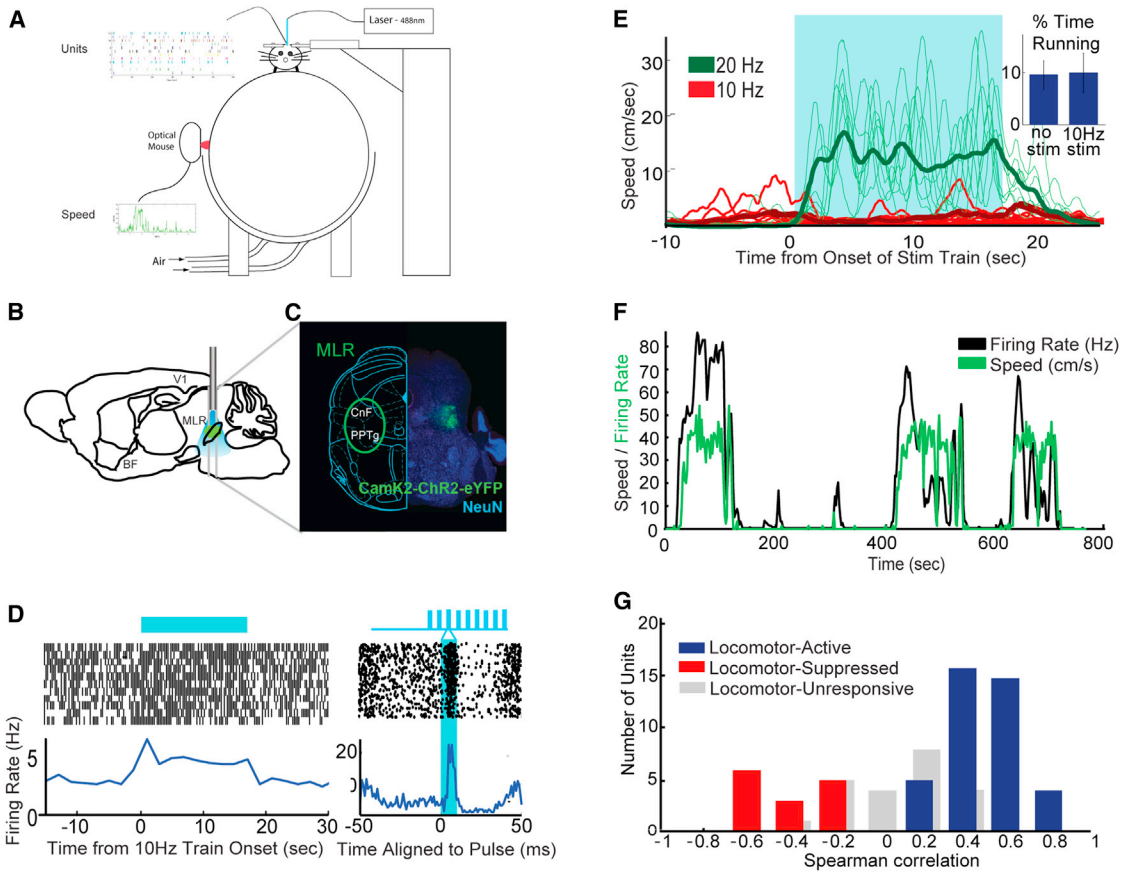

Figure 1. Activation of Neurons within the MLR Induces Locomotion, and MLR Single Units Correlate with Locomotion

(A) Schematic of experimental setup. A mouse is head fixed but free to spontaneously run on a spherical treadmill with sensors to register its locomotor speed.

(B) A multisite electrode with attached optical fiber was lowered into the mesencephalic locomotor region (MLR) to simultaneously optogenetically stimulate neurons and record single-unit responses in experimental subjects injected at least 1 month prior with AAV5-CamK2-ChR2-eYFP into the MLR.

(C) Coronal section demonstrating the extent of infection in the MLR. General extent of MLR is delineated in green. Abbreviations: Cnf, cuneiform nucleus; PPTg, pedunculopontine tegmental nucleus.

(D) Single-unit recordings from a putative optogenetically activated neuron. Rasters and poststimulus time histograms are aligned to the onset of a 10 Hz train of 10 ms light pulse (left) as well as individual pulses (right).

(E) Locomotor speed of an animal while being stimulated in the MLR at 10 Hz (red) or 20 Hz (green) in a head-fixed preparation. Average speed is depicted with bold lines while speeds for individual trains are depicted in thin lines. Proportion of time spent running with and without optical stimulation at 10 Hz (right inset).

(F) Example of the firing rate of a single unit (black) and the locomotor speed of the animal (green) over the course of a recording session.

(G) Peak Spearman's correlation coefficient between firing rate and locomotor speed for the population of units recorded from the MLR. Units were deemed unresponsive if the correlation value was not significantly different from a shuffled distribution of correlations obtained at all lags between firing rates and speeds.

counted). This suggests that glutamatergic projection neurons were preferentially targeted using our viral approach.

In order to determine whether the MLR neurons in the region targeted for optogenetic stimulation were also active during natural locomotion, we recorded their activity in the absence of ChR2 stimulation. In general, their activity was either correlated or anticorrelated with locomotion (Figures 1F and 1G). To quantify these changes, we plotted the Spearman correlation coefficient between running speed and firing rate of MLR units (Figure 1G). Fifty-three percent of recorded units had firing rates that were significantly positively correlated with locomotor speed within a window of 5 s. Eighteen percent had firing rates that were significantly negatively correlated with locomotion, and the remainders were insignificantly correlated with speed based upon our recordings. Thus, activation of units within the MLR is sufficient to induce locomotion, and the activity of a majority of units within the MLR was generally correlated with locomotor speed.

MLR Stimulation Reproduces and Occludes the Effects of Locomotion on Cortex

We studied the effect of MLR stimulation on cortical processing in V1 using the same head-fixed preparation, by making a small craniotomy for insertion of a silicon multisite electrode into visual cortex for the recording of local field potentials and single-unit activity (Figure 2A). This preparation allowed us to measure V1 activity under four conditions: when the animal was stationary or running, each with or without optogenetic activation of the MLR.

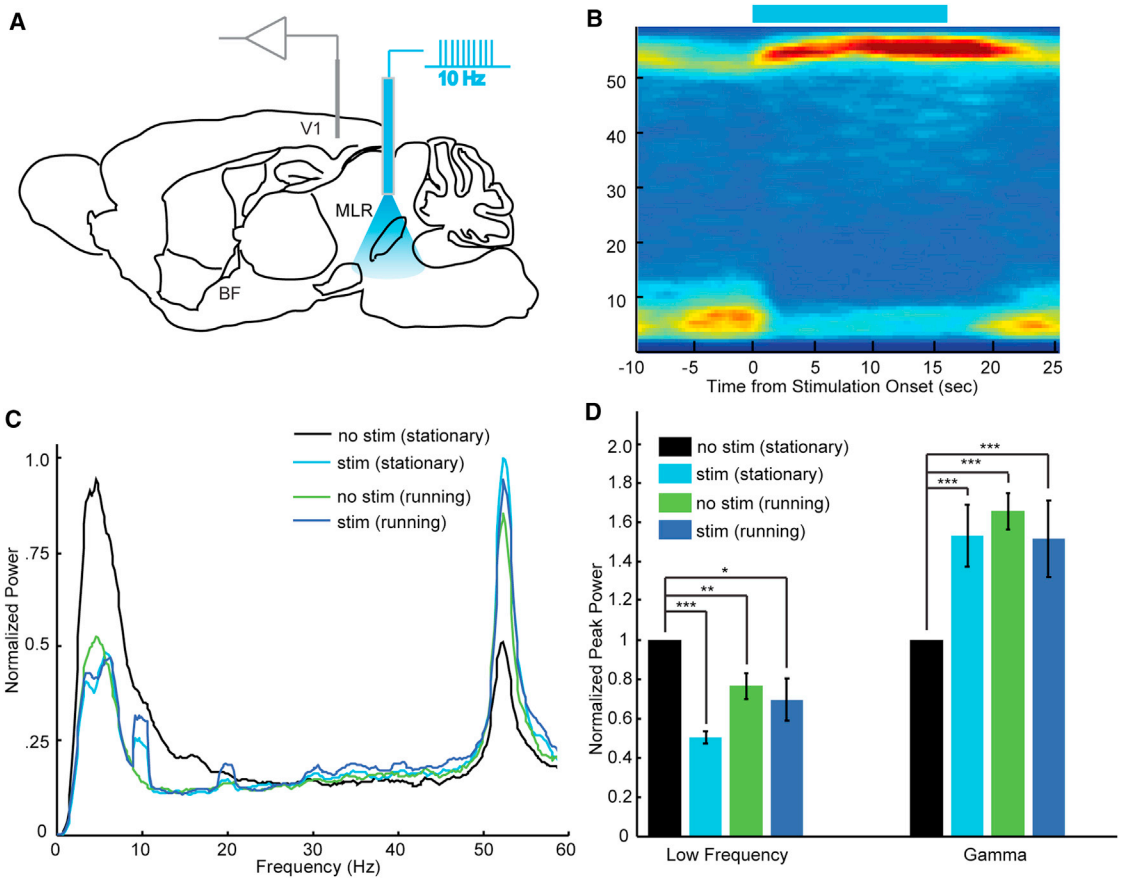

Figure 2. Optical Stimulation of the MLR Induces Changes in LFP Oscillations Similar to Locomotion

(A) Schematic of the experimental setup with a recording array in V1 and optical fiber above the MLR for delivery of 10 Hz optogenetic stimulation into the MLR.

(B) Spectrogram of LFP power across time aligned to the onset of optogenetic stimulation in stationary mouse.

(C) Example of LFP power across various frequencies in the presence/absence of optical stimulation while the animal was stationary or running.

(D) Population summary of median normalized LFP power in the presence/absence of optical stimulation when the animal was stationary or running. LFP power for all conditions is normalized to the LFP power when the animal was stationary and not stimulated. (n = 19 sites from 4 animals). Population values are medians and error bars indicate SEM. p values are reported for paired Wilcoxon signed-rank test. **p < 0.01; ***p < 0.001 using a paired rank-sum test after Bonferroni correction for multiple comparisons.

With no optogenetic stimulation, an increase in high-frequency gamma oscillations and a decrease in low-frequency power was observed in the LFP during periods of locomotion compared to periods when the animal was stationary, as found previously (Niell and Stryker, 2010). This increase in the high-frequency band occurred abruptly upon the initiation of locomotion and was present throughout bouts of movement, suggesting a transition into a different cortical state.

During optogenetic stimulation of the MLR below the threshold for eliciting movement, a similar increase in gamma power was observed, accompanied by the expected decrease in the low-frequency band within LFP (Figure 2B). This pattern of LFP changes mimicked the effects of locomotion on cortical state even though the animal was stationary (Figure 2C) and was observed in all animals (n = 4 animals) (Figure 2D). The peak frequency of the gamma band was similar with or without stimulation (Figure S2A), whereas the peak frequency of low-frequency oscillations shifted slightly toward theta frequencies during stimulation (Figure S2B). Moreover, the enhancement of gamma power and desynchronization of low-frequency power accompanying locomotion occluded any further effects of MLR stimulation, as MLR stimulation caused no significant change in gamma or low-frequency power during periods of running (Figures 2C and 2D).

To investigate the effect of MLR activation on visual responses, we studied single units recorded in V1 across layers using the multisite silicon electrodes during presentation of visual stimuli. Visual responses were evoked using a sinusoidally contrast-modulated white noise stimulus, which cycles from a gray screen up to full contrast and then back down to gray over a 10 s period (Niell and Stryker, 2008) (Figure 3A). This stimulus allowed us to measure average firing rates of isolated single units as well as to make a rapid estimate of contrast-response functions.

We first confirmed that locomotion led to enhanced visually evoked firing rates with very little change in the spontaneous

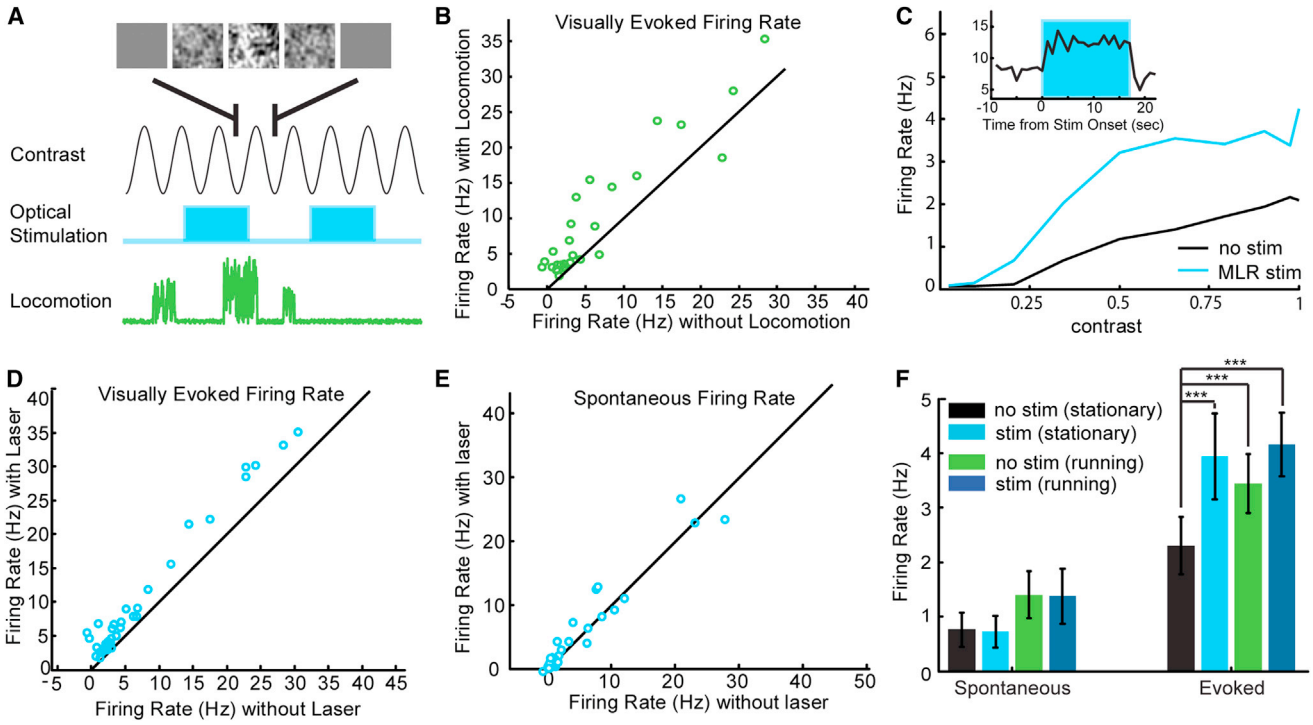

Figure 3. Optical Stimulation of the MLR Increases the Visually Evoked Responses of Neurons in V1

(A) Schematic of experimental setup for the timing of the visual stimuli, optical stimulation, and spontaneous locomotion.

(B) Summary of the visually evoked firing rate for all single units during periods when the animal is running versus stationary.

(C) Example of a single-unit contrast response function, in the presence or absence of optical stimulation, while the animal was stationary. Inset: firing rate for an example single unit averaged across various white noise contrast levels during optogenetic stimulation (blue shaded area).

(D) Visually evoked firing rate of all single units in the presence or absence of optogenetic stimulation while animal was stationary (n = 45 units in 4 animals).

(E) Spontaneous firing rate of all single units during periods in the presence or absence of optogenetic stimulation while the animal was stationary.

(F) Population summary of spontaneous and visually evoked firing rates of single units in the presence or absence of optogenetic stimulation when the animal was either running/stationary. Population values are medians and error bars indicate SEM. p values are reported for paired Wilcoxon signed-rank test. ***p<.001 after Bonferroni correction for multiple comparisons.

firing rates (Figure 3B), consistent with previous studies (Niell and Stryker, 2010). We then recorded the neural responses to contrast-modulated noise movies during epochs with or without optogenetic MLR stimulation. We focused our initial analysis on periods in which the animals were stationary. Similar to locomotion, MLR stimulation significantly increased firing rates rapidly upon the onset of stimulation (Figure 3C, inset). MLR stimulation also increased the slope of the contrast-response function of single units (Figure 3C). Assuming a simple linear relationship between contrast and firing rate, MLR stimulation enhanced the median slope of the contrast-response function by 39% ± 5% in stationary animals ($p < 0.005$ after Bonferroni correction), which was comparable to the gain change with running (56% ± 11%; $p < 0.005$ after Bonferroni correction). This enhancement of visual responses could be observed across the population of responsive neurons (Figure 3D; n = 45 units in 4 mice). In addition, MLR stimulation produced a small but nonsignificant change in the spontaneous firing rate (Figure 3E). Thus, MLR stimulation below the threshold for overt movements qualitatively recapitulated the known effects of locomotion on sensory responses in visual cortex. Additionally, there was no further enhancement of visual responses by running during optogenetic stimulation, suggesting that the effects of MLR activation and locomotion effectively occlude one another and share a common mechanism (Figure 3F). In order to determine whether MLR stimulation preserves response selectivity while enhancing the gain of responses, as previously described for running (Niell and Stryker, 2010), visual responses in a smaller number of experiments were evoked with drifting gratings of various orientations and spatial frequencies (Figures 4A and 4B). Indeed, MLR stimulation below the threshold for overt locomotion did not significantly alter orientation selectivity but enhanced visual responsiveness to a similar extent as previous reports (Figures 4C and 4D). Notably, the enhanced visual responses with MLR stimulation was greater for the visual presentation of drifting gratings than for contrast-modulated white noise, suggesting that these effects can be dependent on the nature of the visual stimulus, consistent with previous findings on locomotion and spatial integration (Ayaz et al., 2013).

In a subset of experiments, optical stimulation within the MLR failed to elicit locomotion at light powers of 20 mW, which was substantially higher than the range of light powers that typically evoked locomotion (up to 5 mW). Upon post hoc histology, it

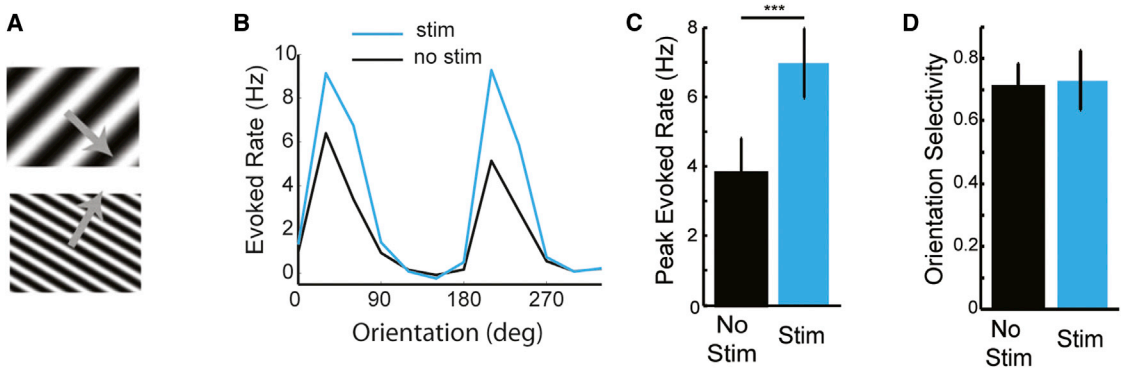

Figure 4. Optical Stimulation in MLR Enhances Responses to Drifting Gratings but Does Not Alter Orientation Selectivity

(A) Drifting gratings of multiple orientations and spatial frequencies were presented during recordings in V1 and optogenetic stimulation of the MLR.

(B) Representative tuning curve without (black) and with (blue) laser stimulation in MLR, in the absence of locomotion.

(C) Increase in peak-evoked response to drifting gratings during laser stimulation.

(D) No change in orientation selectivity of units during laser stimulation. n = 37 units from 3 animals. Error bars represent SEM.

was found that neurons were not infected or infection was outside the region of the cuneiform nucleus and PPN associated with the MLR. In these experiments, optical pulses in the brainstem without activation of MLR neurons failed to elicit any changes in either low-frequency or gamma LFP power while the animal was stationary (Figure S3A). Likewise, there were no changes in either spontaneous or visually evoked firing rates in V1 with the trains of light pulses (Figure S3B). These data suggest that the effect of optogenetic stimulation in the MLR is attributable to the activation of MLR neurons and not the presence of light within the brainstem.

Stimulation of MLR Terminals in the Basal Forebrain Partially Reproduces and Occludes Effects of Locomotion

Previous anatomical and functional studies have demonstrated that the MLR makes a dense projection to the basal forebrain, in addition to its descending motor efferent projections (Dringenberg and Olmstead, 2003; Martinez-Gonzalez et al., 2011). To confirm the presence of these ascending projections, we performed histology on mice injected with AAV-CamK2-ChR2-eYFP into the region of the MLR. After verifying the injection site within the MLR, we examined coronal sections in the region of the basal forebrain, where we found a dense terminal field (Figure 5A, top).

Immunohistochemical staining for choline acetyltransferase (ChAT) revealed large numbers of ChR2-eYFP-labeled projections in the vicinity of cholinergic neurons of the basal forebrain (Figure 5A, bottom), consistent with previous reports (Dringenberg and Olmstead, 2003; Hallanger and Wainer, 1988). In addition to projection to neurons of the cholinergic basal forebrain system such as the nucleus basalis, medial septum, and horizontal diagonal band of Broca, projections could be found in other basal forebrain nuclei such as the extended amygdala complex, substantia inominata, as well as the lateral hypothalamus (Figure S4A). Interestingly, these regions have all been implicated in mediating changes in behavioral state in the context of sleep/wake transition and regulating the theta rhythm.

We next sought to determine whether this projection might mediate the effects of MLR on cortex, by directly stimulating the ChR2-expressing MLR axon terminals in the basal forebrain. At the start of each experiment, short-latency locomotor responses were elicited upon direct optical stimulation at the site of viral infection to verify expression of ChR2-eYFP within the MLR. The fiber optic stimulator was next moved to the basal forebrain to stimulate MLR terminals in the region. A range of peak powers was utilized, spanning 5 to 15 mW. Such optogenetic stimulation usually increased exploratory whisking and sniffing, consistent with previous reports of basal forebrain stimulation (Berg et al., 2005). In this respect, the effect of optogenetic stimulation of MLR terminals in the basal forebrain differed from stimulation of the MLR cell bodies, where whisking and sniffing were accompanied by locomotion. Stimulation of MLR terminals in the basal forebrain did occasionally induce increased locomotion, but the onset of locomotion in these cases was delayed compared to that elicited by direct optogenetic activation of the MLR (Figure S4B).

We then recorded LFP and single-unit responses in V1 while presenting the contrast-modulated white noise movies. Stimulation of MLR projections to the basal forebrain enhanced the power at gamma frequencies while decreasing the power of low-frequency oscillations even in the absence of locomotion (Figure 5B). The peak frequency for gamma and low-frequency oscillations was similar during periods with and without MLR stimulation (Figures S2C and S2D). In addition, locomotion partially occluded the effects of stimulating MLR terminals in the basal forebrain on gamma and low-frequency power as there was no additional increase in gamma power with running (Figure 5B).

We next analyzed the single-unit responses as a function of contrast level with and without stimulation of MLR terminals in the basal forebrain. Optogenetic stimulation enhanced the visually evoked firing rate of V1 neurons (Figure 5C) with rapid onset (Figure S4D). To quantify this, we plotted the visually evoked responses with and without stimulation of MLR terminals to the basal forebrain and observed a significant increase in the visually evoked firing rate across the population (Figure 5C). In contrast,

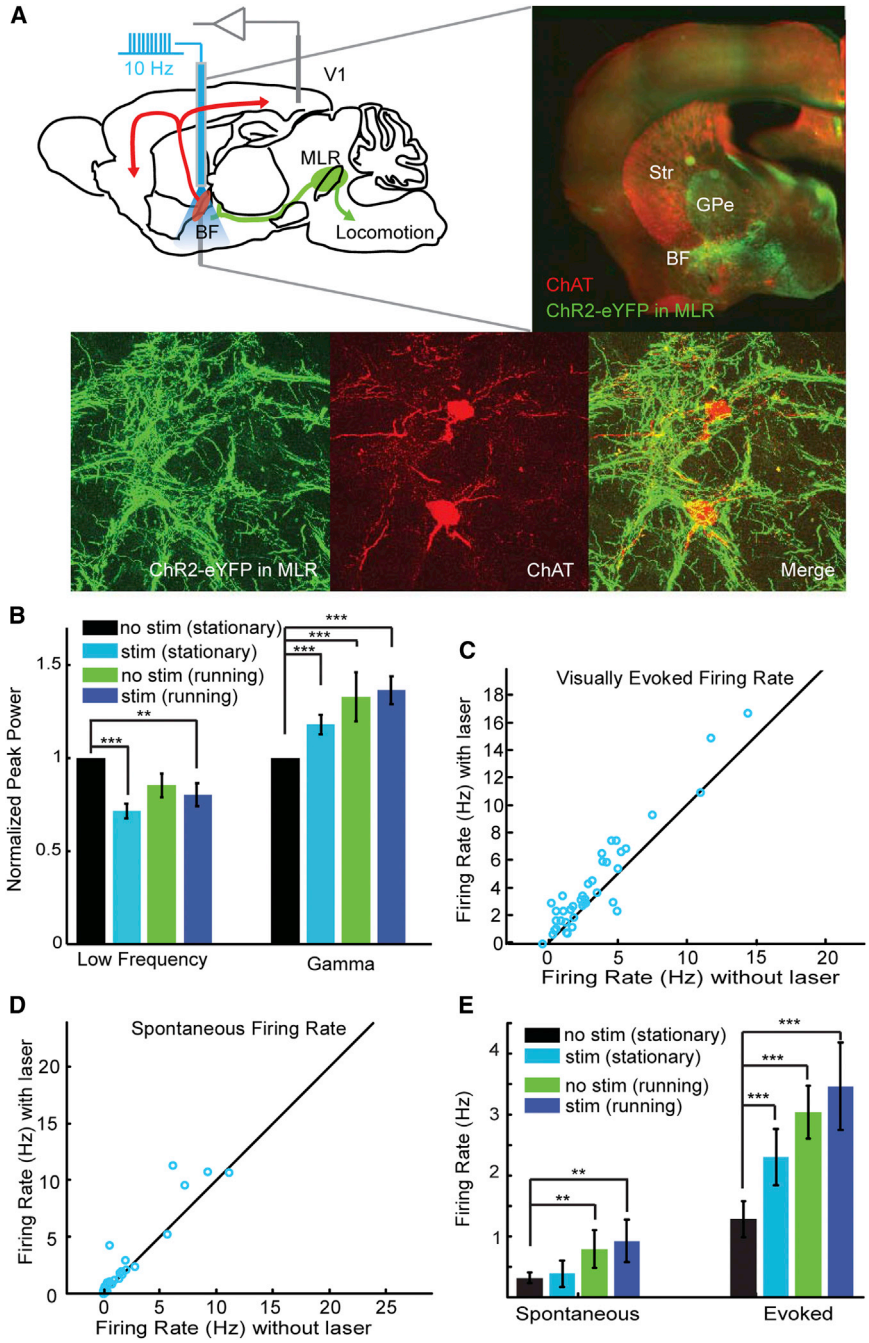

Figure 5. Optogenetic Stimulation of MLR Terminals in the Basal Forebrain Mimics the Effects of Locomotion on Cortex

(A) Schematic of the experimental setup illustrated on a sagittal brain section (top left). Animals were infected with AAV-CamK2-ChR2-eYFP in the MLR at least 1 month prior, allowing for ChR2-eYFP expression in ascending projections from MLR neurons (green) to cholinergic basal forebrain (red). Coronal histological sections of the basal forebrain confirm the presence of ascending projections from the MLR (eYFP) within cholinergic basal forebrain as defined by CHAT (red). Confocal images of MLR terminal fields (green), ChAT immune-stained cells (red) of the nucleus basalis, and the merged image (bottom). Recordings were performed in V1 while simultaneously delivering 10 Hz optical stimulation to ascending projections from the MLR to the basal forebrain.

(B) Population summary of changes in low-frequency and gamma power in the presence/absence of optical stimulation and during periods when the animal is stationary or running (n = 47 sites in 5 animals).

(C) Summary of the visually evoked firing rate of single units during stationary periods in the presence/absence of laser stimulation (n = 60 units in 5 animals).

(D) Summary of the spontaneous firing rate of neurons during stationary periods in the presence/absence of laser stimulation.

(E) Summary of the spontaneous and visually evoked firing rate of neurons during periods when an animal is stationary or running in the presence/absence of laser stimulation. Population data represents medians, and error bars indicate SEM. p values are reported for paired Wilcoxon signed-rank test. **p < 0.01; ***p < 0.001 after Bonferroni correction for multiple comparisons.

the spontaneous firing rates of V1 units were modestly, but significantly, changed during optogenetic stimulation of MLR inputs to the basal forebrain (Figure 5D). MLR terminal stimulation during epochs when the animal was stationary produced an enhancement of visually evoked responses, which resembled changes in responsiveness observed during locomotion (Figure S4E). Locomotion caused only a small nonsignificant increase in the firing rate during optogenetic stimulation, indicating that the effects of locomotion were largely occluded by terminal stimulation (Figure 5E). These findings suggest that the MLR may mediate its effect on cortex in part via projections to basal forebrain, consistent with other studies demonstrating a role for basal forebrain in shifts in cortical state (Pinto et al., 2013; Fu et al., 2014).

DISCUSSION

Previous studies have demonstrated that locomotor activity can dramatically change the responsiveness of mouse V1 to visual stimuli (Ayaz et al., 2013; Keller et al., 2012; Niell and Stryker, 2010). Here, we provide evidence for a brainstem circuit that initiates and couples locomotion with changes in cortical state via ascending and descending projections from the MLR (Figure 5A). We demonstrate that activating the ascending pathway from the MLR, without fully recruiting the descending locomotor outputs, recapitulates the changes in the responsiveness of V1 that are associated with locomotion.

MLR Couples Changes in Brain States with Locomotion

The MLR has been studied in numerous contexts and reports on it have used a variety of nomenclatures (Martinez-Gonzalez et al., 2011), confounding attempts to identify a unitary function of this brain region. Here, we have chosen to describe this region as the MLR defined functionally as the area in the midbrain where locomotion can be initiated at short latencies by stimulation (Grillner et al., 2008; Mori et al., 1978). However, the MLR is coextensive with the PPN, the limits of which are histochemically defined by the presence of cholinergic neurons in the dorsal midbrain tegmentum (Martinez-Gonzalez et al., 2011; Thankachan et al., 2012). In the sleep literature, numerous studies have implicated the PPN in sleep-wake regulation (Rye, 1997).

An alternative nomenclature that is used to describe this pontine tegmental area is the parabrachial region, due to its close proximity to the brachium conjuctivum. In anesthetized animals, stimulation of the parabrachial region has been documented as regulating behavioral signs and electrophysiological correlates of alertness across the brain and therefore has been described as being a part of the ascending reticular activating system (“ARAS”) (French et al., 1952; Moruzzi and Magoun, 1949). Stimulation of the parabrachial region has been found to (1) “desynchronize” low-frequency oscillations and increase gamma power in the cortex (Munk et al., 1996), (2) promote a transition from burst to tonic firing modes in the thalamus (Lu et al., 1993), and (3) increase the power and frequency of theta oscillations in the hippocampus of anesthetized animals (Pignatelli et al., 2012). Because these studies were conducted in anesthetized animals, it was not possible to assay the animals’ behavior during stimulation.

While the locomotor and electrophysiological changes resulting from stimulation have been independently documented and are seemingly unrelated, these findings can be reconciled by a simple model in which the MLR initiates locomotion through descending pathways to the spinal cord while coordinating changes in brain state through its ascending projections (Figure 5A). Here, we have shown that activation of projections from the MLR to the basal forebrain is sufficient to mimic the changes in visual cortical processing observed with locomotion. The MLR also provides direct cholinergic neuromodulatory input to the thalamus (Erişir et al., 1997), facilitating burst-to-tonic transitions in firing (Curró Dossi et al., 1991; Steriade et al., 1991) and projects to the medial septum, which contains central pattern generators for inducing hippocampal theta oscillations (Buzsáki and Moser, 2013; Pignatelli et al., 2012). We speculate that these other ascending projections (Hallanger and Wainer, 1988) may respectively mediate concomitant changes in the thalamus (Niell and Stryker, 2010) and hippocampus (Buzsáki and Moser, 2013) that accompany locomotion. In turn, other regions such as the basal ganglia and brainstem may regulate activity within the MLR and locomotor decisions (Grillner et al., 2008; Kravitz et al., 2010; Tai et al., 2012).

Methodological Considerations

Our experimental design drew upon previous studies in primates utilizing electrical microstimulation to identify a role for brain regions controlling saccadic eye movements in spatial attention. In these studies, electrical stimulation below the threshold for overt motor behavior could reproduce changes in sensory responses associated with spatial attention (Moore and Armstrong, 2003; Müller et al., 2005). Here, we used optogenetic stimulation to identify the MLR and identified a similar role for this region in regulating sensory responses.

However, optogenetic stimulation afforded several benefits over traditional electrical microstimulation. One benefit is that we could identify the neuronal cell bodies that were being activated. This is in contrast to electrical stimulation, which may recruit activity from axons of passage and give rise to both orthodromic and antidromic activation (Histed et al., 2009). The viral approach we utilized preferentially targeted glutamatergic neurons (Figure S1B) within the heterogeneous MLR, which contains cholinergic, glutamatergic, and GABAergic subpopulations of neurons (Martinez-Gonzalez et al., 2011; Thankachan et al., 2012). Glutamatergic neurons send long-range projections, including descending projections to locomotor regions and ascending projections to multiple areas, making them ideally suited to couple locomotion and state changes. Further efforts will be required to identify the specific contributions of the multiple cell types. Lastly, we were able to perform stimulation of MLR projections to the basal forebrain, which appeared sufficient to induce increases in V1 responses. While these results are suggestive, it is still possible that optogenetic stimulation directed into the basal forebrain may antidromically activate MLR neurons, which in turn may terminate elsewhere. In this case, stimulation would not necessarily be restricted to a pathway from the MLR to the basal forebrain, but rather would be targeted to a subset of MLR neurons with ascending projections to the basal forebrain and other possible collaterals.

Neural Circuits Coupling Locomotion to Cortical State

Our findings, in conjunction with other recent studies, provide a partial neural circuit describing how locomotion can influence cortical processing. Evidence from decerebrate preparations suggests that the MLR is able to initiate locomotion through descending commands that recruit spinal cord central pattern generators. Here, we provided evidence that the MLR can also influence cortical processing, potentially through projections directed toward the basal forebrain. The changes in cortical state initiated by stimulation of MLR terminals in the basal forebrain resemble those produced by cholinergic neuromodulatory influences of nucleus basalis stimulation on cortex, suggesting a possible pathway by which MLR can influence cortex (Alitto and Dan, 2012; Buzsaki et al., 1988; Goard and Dan, 2009; Hasselmo and Giocomo, 2006; Rodriguez et al., 2004; Sato et al., 1987). In particular, Pinto et al. (2013) demonstrated that optogenetic stimulation of the cholinergic nucleus basalis can decrease cortical coherence and enhance activity in V1, mimicking the effects of locomotion, while inhibition had the opposite effects on cortical processing. Furthermore, Fu et al. (2014) recently provided evidence supporting a general cortical microcircuit whereby cholinergic input to VIP interneurons communicates locomotor-related information. VIP interneurons in turn inhibit SST-positive interneurons to disinhibit neighboring excitatory neurons. Together, these studies and our current data are consistent with a model in which the MLR provides the basal forebrain with an efference copy of locomotor signals to regulate

cortical state through cholinergic neuromodulation and local microcircuitry.

However, it is also likely that locomotion can affect processing in V1 by additional routes. For instance, Polack et al. (2013) demonstrate that noradrenergic input mediates tonic depolarization of excitatory neurons during running. By bringing the membrane potential of principal neurons closer to threshold, noradrenergic neuromodulation from the locus coeruleus is likely to contribute to enhanced visual responses during locomotion. It remains unclear whether the MLR can also directly or indirectly regulate the activity of neurons within the locus coruleus (Foote et al., 1980).

Implication for Self-Reported Increase in "Alertness" during Therapeutic PPN Stimulation

The PPN, the human homolog of the MLR, has been targeted as a site for DBS in Parkinson's patients to relieve the freezing of gait and postural instability, which are cardinal features of the disorder (Hamani et al., 2011; Stefani et al., 2007). Surprisingly, however, numerous studies have described that patients often feel subjectively more "alert" upon the onset of low-frequency (15–25 Hz) DBS in the PPN (Stefani et al., 2013). Our data can provide a potential explanation for these findings, demonstrating that the MLR/PPN mediates both locomotion as well as changes in behavioral state that are naturally recruited in tandem. Both the desynchronization of low-frequency oscillations and the concomitant increase in gamma oscillations have been described as electrophysiological correlates of an "alert" behavioral state (Harris and Thiele, 2011). An increase in the gain of sensory-evoked responses is also consistent with an "alert" state. Thus, it is reasonable to infer that the subjective sense of "alertness" felt by patients during low-frequency DBS in the PPN may be due to the PPN's ascending efferents to neuromodulatory centers, including the cholinergic neurons of the basal forebrain. These clinical studies are interesting in that they help address questions that are difficult to assay in animal models because patients can subjectively report their changes in perception. The animal models complement the clinical observations by providing potential mechanistic explanations of the changes associated with clinical interventions.

The present experiments imply that the MLR has a dual function, concurrently regulating both locomotion and brain state. The MLR's projection to the basal forebrain may account for other recent findings of changes associated with locomotion in extrastriate visual cortex (Andermann et al., 2011), auditory cortex (Zhou et al., 2014), and hippocampus (Ahmed and Mehta, 2012; Kemere et al., 2013). Thus, while these systems are affected differently by locomotion, we hypothesize that this diversity may share a common mechanism mediated by ascending projections from the MLR. Continued optogenetic dissection of these circuits may reveal the full map of connections that can mediate the effects of behavioral state on higher brain functions.

EXPERIMENTAL PROCEDURES

Mice

Mice were maintained in the animal facility at University of Oregon, the Ernest Gallo Clinic and Research Center, and the University of California, San Francisco and used in accordance with protocols approved by the University of Oregon, Ernest Gallo Clinic and Research Center, and the University of California, San Francisco Institutional Animal Care and Use Committees. Experiments were performed on adult C57Bl/6 mice (age 2–6 months, both male and female).

Virus Preparation

The pAAV-CamK2α-ChR2(H124R)-eYFP construct was obtained from K. Deisseroth (Stanford University) and used for production of AAV serotype 2/5 by the viral core at University of North Carolina. The final concentration was 1–2 × 10^{12} viral particles per ml.

Stereotaxic AAV Injection

Animals were anesthetized with either ketamine (150 mg/kg) and xylazine (50 mg/kg) or 2% isoflurane (vol/vol) gas anesthesia. Animals were placed in a stereotaxic frame and 26G microinjection needles were inserted through a burr hole bilaterally into the MLR (coordinates from bregma: −4.75 mm anterior, ± 1.2 mm medial-lateral, –3.6 ventral). We performed 0.5 μl injections using a 1 μl Hamilton syringe through a hydraulic pump (Harvard Instruments) and the injections took place over 5 min followed by 5 min of recovery. We then allowed at least a month before recording to allow full ChR2 expression.

Surgical Preparation

Surgical preparation and recordings were performed generally as described previously (Niell and Stryker, 2010). Briefly, in preparation for recording, a metal headplate was affixed to the skull with cyanoacrylate and dental acrylic. After allowing several days for recovery, in a second surgery on the morning of recording, we performed a small craniotomy (~1 mm) centered over V1 and made a burr hole over the site of the viral injection and/or the basal forebrain (coordinates from bregma: −0.5 mm anterior, ± 1.75 mm medial-lateral, –3.75 ventral). The headplate opening was then filled with silicone elastomer, and the animal was allowed to recover for 2–3 hr before recording. After recovery, the animal was placed in the head holder on the floating ball and the silicone plug was removed.

Optical Stimulation

To stimulate activity in the MLR, the tip of a 200 μm fiber optic was lowered into the burr hole until it was 0.5 mm above the site of viral injection. The fiber optic was covered in furcation tubing to protect the fiber and to prevent light from escaping through the optic-patch cord. A 473 nm diode-pumped solid-state laser (OEM Laser Systems, 200 mW) provided the light stimulation. The laser driver current was adjusted to induce overt locomotion by 10 ms pulses of light at 20 Hz but no locomotion at the same intensity and pulse duration at 10 Hz frequency. For subsequent experiments, stimulation was delivered at 10 Hz during visual presentation for a period of 17 s, and 17 s was allowed to elapse between trains of stimulation. For experiments involving stimulation of MLR terminals in BF, following confirmation that stimulation in the MLR could induce movement, we moved the fiber to the burr hole over BF, lowered to a depth of 3.5–4 mm, and used a similar stimulation protocol.

Extracellular Single-Unit Recordings

We used silicon multisite electrodes, following the methods of Niell and Stryker (2010), to record single-unit activity in cortex during locomotion and optogenetic stimulation. Briefly, the silicon probe (a1 × 32–25-5 mm-177, NeuroNexus Technologies) was lowered through the craniotomy using a stereotax-mounted Microdrive (Siskiyou Designs). The electrode was placed at an angle of ~45° relative to the cortical surface and inserted to a depth of up to 800 μm below the cortical surface to record cells across multiple layers.

The electrode was placed without regard for the presence of visually responsive units on individual sites, and all units stably isolated over the recording period were included in analysis. Following placement, the electrode was embedded in agarose to increase mechanical stability and was allowed to settle in one position for 30 min to obtain stable single-unit recordings. Recordings continued for up to several hours, after which the animal was euthanized under deep anesthesia by cervical dislocation. The brain was removed immediately and fixed by immersion in 4% paraformaldehyde in PBS at 4°C overnight, after which 200 μm coronal sections were cut with a vibratome. The

sections were mounted using Vectashield with DAPI (Vector Laboratories) and imaged on an Olympus BX6l microscope to confirm viral expression in the MLR.

Visual Stimuli

Visual stimuli were presented as described previously (Niell and Stryker, 2008). Briefly, stimuli were generated in MATLAB using the Psychophysics Toolbox extensions (Brainard, 1997; Pelli, 1997) and displayed with gamma correction on a monitor (Planar SA2311W, 30 × 50 cm, 60 Hz refresh rate) placed 25 cm from the mouse, subtending approximately 60°–75° of visual space. Contrast-modulated noise movies (Niell and Stryker, 2008) were created by first generating a random spatiotemporal frequency spectrum in the Fourier domain with defined spectral characteristics. To drive as many simultaneously recorded units as possible, we used a spatial frequency spectrum that dropped off as $A(f) \sim 1/(f + fc)$, with $fc = 0.05$ cpd, and a sharp cutoff at 0.12 cpd, to approximately match the stimulus energy to the distribution of spatial frequency preferences. The temporal frequency spectrum was flat with a sharp low-pass cutoff at 5 Hz. This 3D (ωx, ωy, ωt) spectrum was then inverted to generate a spatiotemporal movie. To provide contrast modulation, we multiplied this movie by a sinusoidally varying contrast with 10 s period. Each movie was 5 min long and was repeated two or three times, for 10–15 min total presentation.

In a subset of experiments, we presented drifting sinusoidal gratings as described previously (Niell and Stryker, 2010) in 12 directions of motion and six spatial frequencies (0.01 – 0.32 cpd) at 2 Hz temporal frequency. Each stimulus was presented in randomly interleaved order for 1.5 s, with 0.2 s interstimulus interval.

Data Acquisition

Data acquisition was performed as described by Niell and Stryker (2010). Signals were acquired using a System 3 workstation (Tucker-Davis Technologies) and analyzed with custom software in MATLAB (MathWorks). For LFP analysis, the extracellular signal was filtered from 1 to 300 Hz and sampled at 1.5 kHz. To obtain single-unit activity, we filtered the extracellular signal from 0.7 to 7 kHz and sampled at 25 kHz. Spiking events were detected online by voltage threshold crossing, and a 1 ms waveform sample on four neighboring recording sites was acquired around the time of threshold crossing. Single-unit clustering and spike waveform analysis were performed as described previously (Niell and Stryker, 2008), with a combination of custom software in MATLAB and Klusta-Kwik (Harris et al., 2000). Quality of separation was determined based on the Mahalanobis distance and L-ratio (Schmitzer-Torbert et al., 2005) and evidence of a clear refractory period. Units were also checked for stability in terms of amplitude and waveform over the course of the recording time to ensure that they had not drifted or suffered mechanical damage.

Movement signals from the optical mice were acquired in an event-driven mode at up to 300 Hz and integrated at 100 ms intervals. These measurements were used to calculate the net physical displacement of the top surface of the ball. We determined the average speed during a stimulus presentation to classify the trial as stationary (<1 cm/s) or moving (>1 cm/s).

Data Analysis

Data analysis was performed using custom routines written in MATLAB. To analyze visual responsiveness using contrast-modulated white-noise movies, we binned the spikes of each neuron according to the contrast of the movie on the screen, to create a contrast-response function. The spontaneous firing rate was defined as the firing rate for zero contrast, while evoked firing rate was defined as firing for period within 80% of full contrast or greater. To calculate responsiveness as a function of locomotor state or laser stimulation on/off, we simply performed this analysis after filtering the time point of each spike for the appropriate criteria.

Drifting grating responses were analyzed according to Niell and Stryker (2010), by fitting a sum of Gaussians to the orientation tuning curve at the peak spatial frequency. This was performed separately for trials when the animal was stationary or moving.

For LFP analysis, the power spectrum was computed using multitaper estimation in MATLAB with the Chronux package (http://chronux.org/) (Mitra and Bokil, 2007), using a 3 s sliding window at 1 s intervals, with three to five tapers. As described previously (Niell and Stryker, 2010), spectra were normalized for presentation by applying a 1/f correction (Sirota et al., 2008). An alternative presentation method, using a log scale without 1/f normalization, is demonstrated in Figure S2E and shows the same peaks. To compare power in different frequency ranges across states, we selected all the 1 s time windows meeting a certain criteria (laser on/off, moving/stationary), averaged the LFP spectrum, and found the peak of power within the appropriate frequency range. Frequencies at a multiple of the laser stimulation frequency were excluded from this analysis to avoid including harmonics.

Statistical significance was determined by Mann-Whitney U test, except where otherwise stated. For figures representing the median of data, error bars indicate SE of the median as calculated by a bootstrap.

SUPPLEMENTAL INFORMATION

Supplemental Information includes four figures and one movie and can be found with this article online at http://dx.doi.org/10.1016/j.neuron.2014.06.031.

ACKNOWLEDGMENTS

This work was supported by NIH Grants 1R01EY023337 (to C.M.N.), 1R01EY02874 (to M.P.S.), and 1RC2NS069350 and 1R01MH087542 (to L.W.), and the State of California. We thank Dr. Loren Frank, Dr. Denise Piscopo, and Dr. Michael Wehr for comments on the manuscript, and members of the L.W., M.P.S., A.B., and C.M.N. labs for insightful discussions.

Accepted: June 12, 2014
Published: July 16, 2014

REFERENCES

Ahmed, O.J., and Mehta, M.R. (2012). Running speed alters the frequency of hippocampal gamma oscillations. J. Neurosci. *32*, 7373–7383.

Alitto, H.J., and Dan, Y. (2012). Cell-type-specific modulation of neocortical activity by basal forebrain input. Front. Syst. Neurosci. *6*, 79.

Andermann, M.L., Kerlin, A.M., Roumis, D.K., Glickfeld, L.L., and Reid, R.C. (2011). Functional specialization of mouse higher visual cortical areas. Neuron *72*, 1025–1039.

Armstrong, K.M., Fitzgerald, J.K., and Moore, T. (2006). Changes in visual receptive fields with microstimulation of frontal cortex. Neuron *50*, 791–798.

Ayaz, A., Saleem, A.B., Schölvinck, M.L., and Carandini, M. (2013). Locomotion controls spatial integration in mouse visual cortex. Curr. Biol. *23*, 890–894.

Bennett, C., Arroyo, S., and Hestrin, S. (2013). Subthreshold mechanisms underlying state-dependent modulation of visual responses. Neuron *80*, 350–357.

Berg, R.W., Friedman, B., Schroeder, L.F., and Kleinfeld, D. (2005). Activation of nucleus basalis facilitates cortical control of a brain stem motor program. J. Neurophysiol. *94*, 699–711.

Bisley, J.W. (2011). The neural basis of visual attention. J. Physiol. *589*, 49–57.

Brainard, D.H. (1997). The Psychophysics Toolbox. Spat. Vis. *10*, 433–436.

Buzsáki, G., and Moser, E.I. (2013). Memory, navigation and theta rhythm in the hippocampal-entorhinal system. Nat. Neurosci. *16*, 130–138.

Buzsaki, G., Bickford, R.G., Ponomareff, G., Thal, L.J., Mandel, R., and Gage, F.H. (1988). Nucleus basalis and thalamic control of neocortical activity in the freely moving rat. J. Neurosci. *8*, 4007–4026.

Cavanaugh, J., and Wurtz, R.H. (2004). Subcortical modulation of attention counters change blindness. J. Neurosci. *24*, 11236–11243.

Curró Dossi, R., Paré, D., and Steriade, M. (1991). Short-lasting nicotinic and long-lasting muscarinic depolarizing responses of thalamocortical neurons to stimulation of mesopontine cholinergic nuclei. J. Neurophysiol. *65*, 393–406.

Cutrell, E.B., and Marrocco, R.T. (2002). Electrical microstimulation of primate posterior parietal cortex initiates orienting and alerting components of covert attention. Exp. Brain Res. *144*, 103–113.

Dombeck, D.A., Khabbaz, A.N., Collman, F., Adelman, T.L., and Tank, D.W. (2007). Imaging large-scale neural activity with cellular resolution in awake, mobile mice. Neuron *56*, 43–57.

Dringenberg, H.C., and Olmstead, M.C. (2003). Integrated contributions of basal forebrain and thalamus to neocortical activation elicited by pedunculopontine tegmental stimulation in urethane-anesthetized rats. Neuroscience *119*, 839–853.

Erişir, A., Van Horn, S.C., and Sherman, S.M. (1997). Relative numbers of cortical and brainstem inputs to the lateral geniculate nucleus. Proc. Natl. Acad. Sci. USA *94*, 1517–1520.

Foote, S.L., Aston-Jones, G., and Bloom, F.E. (1980). Impulse activity of locus coeruleus neurons in awake rats and monkeys is a function of sensory stimulation and arousal. Proc. Natl. Acad. Sci. USA *77*, 3033–3037.

French, J.C., Von Amerongen, F.K., and Magoun, H.W. (1952). An activating system in brain stem of monkey. AMA Arch. Neurol. Psychiatry *68*, 577–590.

Fu, Y., Tucciarone, J.M., Espinosa, J.S., Sheng, N., Darcy, D.P., Nicoll, R.A., Huang, Z.J., and Stryker, M.P. (2014). A cortical circuit for gain control by behavioral state. Cell *156*, 1139–1152.

Goard, M., and Dan, Y. (2009). Basal forebrain activation enhances cortical coding of natural scenes. Nat. Neurosci. *12*, 1444–1449.

Gradinaru, V., Mogri, M., Thompson, K.R., Henderson, J.M., and Deisseroth, K. (2009). Optical deconstruction of parkinsonian neural circuitry. Science *324*, 354–359.

Grillner, S. (2003). The motor infrastructure: from ion channels to neuronal networks. Nat. Rev. Neurosci. *4*, 573–586.

Grillner, S., Wallen, P., Saitoh, K., Kozlov, A., and Robertson, B. (2008). Neural bases of goal-directed locomotion in vertebrates–an overview. Brain Res. Rev. *57*, 2–12.

Hallanger, A.E., and Wainer, B.H. (1988). Ascending projections from the pedunculopontine tegmental nucleus and the adjacent mesopontine tegmentum in the rat. J. Comp. Neurol. *274*, 483–515.

Hamani, C., Moro, E., and Lozano, A.M. (2011). The pedunculopontine nucleus as a target for deep brain stimulation. J. Neural Transm. *118*, 1461–1468.

Harris, K.D., and Thiele, A. (2011). Cortical state and attention. Nat. Rev. Neurosci. *12*, 509–523.

Harris, K.D., Henze, D.A., Csicsvari, J., Hirase, H., and Buzsaki, G. (2000). Accuracy of tetrode spike separation as determined by simultaneous intracellular and extracellular measurements. J. Neurophysiol. *84*, 401–414.

Harvey, C.D., Collman, F., Dombeck, D.A., and Tank, D.W. (2009). Intracellular dynamics of hippocampal place cells during virtual navigation. Nature *461*, 941–946.

Hasselmo, M.E., and Giocomo, L.M. (2006). Cholinergic modulation of cortical function. J. Mol. Neurosci. *30*, 133–135.

Histed, M.H., Bonin, V., and Reid, R.C. (2009). Direct activation of sparse, distributed populations of cortical neurons by electrical microstimulation. Neuron *63*, 508–522.

Keller, G.B., Bonhoeffer, T., and Hübener, M. (2012). Sensorimotor mismatch signals in primary visual cortex of the behaving mouse. Neuron *74*, 809–815.

Kemere, C., Carr, M.F., Karlsson, M.P., and Frank, L.M. (2013). Rapid and continuous modulation of hippocampal network state during exploration of new places. PLoS ONE *8*, e73114.

Kravitz, A.V., Freeze, B.S., Parker, P.R., Kay, K., Thwin, M.T., Deisseroth, K., and Kreitzer, A.C. (2010). Regulation of parkinsonian motor behaviours by optogenetic control of basal ganglia circuitry. Nature *466*, 622–626.

Lindsley, D.B., Schreiner, L.H., Knowles, W.B., and Magoun, H.W. (1950). Behavioral and EEG changes following chronic brain stem lesions in the cat. Electroencephalogr. Clin. Neurophysiol. *2*, 483–498.

Lu, S.M., Guido, W., and Sherman, S.M. (1993). The brain-stem parabrachial region controls mode of response to visual stimulation of neurons in the cat's lateral geniculate nucleus. Vis. Neurosci. *10*, 631–642.

Martinez-Gonzalez, C., Bolam, J.P., and Mena-Segovia, J. (2011). Topographical organization of the pedunculopontine nucleus. Front. Neuroanat. *5*, 22.

Mitra, P.P., and Bokil, H. (2007). Observed Brain Dynamics. (Oxford: Oxford University Press).

Moore, T., and Armstrong, K.M. (2003). Selective gating of visual signals by microstimulation of frontal cortex. Nature *421*, 370–373.

Moore, T., and Fallah, M. (2001). Control of eye movements and spatial attention. Proc. Natl. Acad. Sci. USA *98*, 1273–1276.

Mori, S., Nishimura, H., Kurakami, C., Yamamura, T., and Aoki, M. (1978). Controlled locomotion in the mesencephalic cat: distribution of facilitatory and inhibitory regions within pontine tegmentum. J. Neurophysiol. *41*, 1580–1591.

Moruzzi, G., and Magoun, H.W. (1949). Brain stem reticular formation and activation of the EEG. Electroencephalogr. Clin. Neurophysiol. *1*, 455–473.

Müller, J.R., Philiastides, M.G., and Newsome, W.T. (2005). Microstimulation of the superior colliculus focuses attention without moving the eyes. Proc. Natl. Acad. Sci. USA *102*, 524–529.

Munk, M.H., Roelfsema, P.R., König, P., Engel, A.K., and Singer, W. (1996). Role of reticular activation in the modulation of intracortical synchronization. Science *272*, 271–274.

Nauta, W.J.H., and Kuypers, H. (1958). Some ascending pathways in the brain stem reticular formation. In Reticular Formation of the Brain, H.H. Jasper, L.D. Proctor, R.S. Knighton, W.C. Noshay, and R.T. Costello, eds. (Boston: Little, Brown, and Co.), pp. 3–30.

Niell, C.M., and Stryker, M.P. (2008). Highly selective receptive fields in mouse visual cortex. J. Neurosci. *28*, 7520–7536.

Niell, C.M., and Stryker, M.P. (2010). Modulation of visual responses by behavioral state in mouse visual cortex. Neuron *65*, 472–479.

Pelli, D.G. (1997). The VideoToolbox software for visual psychophysics: transforming numbers into movies. Spat. Vis. *10*, 437–442.

Pignatelli, M., Beyeler, A., and Leinekugel, X. (2012). Neural circuits underlying the generation of theta oscillations. J. Physiol. Paris *106*, 81–92.

Pinto, L., Goard, M.J., Estandian, D., Xu, M., Kwan, A.C., Lee, S.H., Harrison, T.C., Feng, G., and Dan, Y. (2013). Fast modulation of visual perception by basal forebrain cholinergic neurons. Nat. Neurosci. *16*, 1857–1863.

Polack, P.O., Friedman, J., and Golshani, P. (2013). Cellular mechanisms of brain state-dependent gain modulation in visual cortex. Nat. Neurosci. *16*, 1331–1339.

Rodriguez, R., Kallenbach, U., Singer, W., and Munk, M.H. (2004). Short- and long-term effects of cholinergic modulation on gamma oscillations and response synchronization in the visual cortex. J. Neurosci. *24*, 10369–10378.

Rye, D.B. (1997). Contributions of the pedunculopontine region to normal and altered REM sleep. Sleep *20*, 757–788.

Sato, H., Hata, Y., Masui, H., and Tsumoto, T. (1987). A functional role of cholinergic innervation to neurons in the cat visual cortex. J. Neurophysiol. *58*, 765–780.

Schmitzer-Torbert, N., Jackson, J., Henze, D., Harris, K., and Redish, A.D. (2005). Quantitative measures of cluster quality for use in extracellular recordings. Neuroscience *131*, 1–11.

Shik, M.L., Severin, F.V., and Orlovskiĭ, G.N. (1966). [Control of walking and running by means of electric stimulation of the midbrain]. Biofizika *11*, 659–666.

Sirota, A., Montgomery, S., Fujisawa, S., Isomura, Y., Zugaro, M., and Buzsaki, G. (2008). Entrainment of neocortical neurons and gamma oscillations by the hippocampal theta rhythm. Neuron *60*, 683–697.

Stefani, A., Lozano, A.M., Peppe, A., Stanzione, P., Galati, S., Tropepi, D., Pierantozzi, M., Brusa, L., Scarnati, E., and Mazzone, P. (2007). Bilateral

deep brain stimulation of the pedunculopontine and subthalamic nuclei in severe Parkinson's disease. Brain *130*, 1596–1607.

Stefani, A., Peppe, A., Galati, S., Bassi, M.S., D'Angelo, V., and Pierantozzi, M. (2013). The serendipity case of the pedunculopontine nucleus low-frequency brain stimulation: chasing a gait response, finding sleep, and cognition improvement. Front. Neurol. *4*, 68.

Steriade, M., Dossi, R.C., Paré, D., and Oakson, G. (1991). Fast oscillations (20-40 Hz) in thalamocortical systems and their potentiation by mesopontine cholinergic nuclei in the cat. Proc. Natl. Acad. Sci. USA *88*, 4396–4400.

Tai, L.H., Lee, A.M., Benavidez, N., Bonci, A., and Wilbrecht, L. (2012). Transient stimulation of distinct subpopulations of striatal neurons mimics changes in action value. Nat. Neurosci. *15*, 1281–1289.

Thankachan, S., Fuller, P.M., and Lu, J. (2012). Movement- and behavioral state-dependent activity of pontine reticulospinal neurons. Neuroscience *221*, 125–139.

Zhou, M., Liang, F., Xiong, X.R., Li, L., Li, H., Xiao, Z., Tao, H.W., and Zhang, L.I. (2014). Scaling down of balanced excitation and inhibition by active behavioral states in auditory cortex. Nat. Neurosci. *17*, 841–850.